PhD thesis

Comparative study of physiological and pathological autoimmune models

Katalin Olasz

Department of Immunology and Biotechnology

University of Pécs, Faculty of Medicine

Project leader: Dr. Ferenc Boldizsár, Prof. Dr. Péter Németh

PhD program leader: Prof. Dr. Péter Németh

Pécs

2012

SUMMARY

The aim of our work was the comparison of physiological and pathological autoimmunity by using two different experimental system: i) detailed analisys of human serum samples searching for natural autoantibodies (nAAb), ii) investigation of possible pathological mechanisms of autoimmunity in a mouse model of rheumatoid arthritis.

We used citrate-synthase (genetically conserved inner membrane enzyme of the mitochondria) as a model antigen for epitope mapping of natural autoantibodies (nAAb). With two different technologies (overlapping decapeptide system and phage-display) we successfully demonstrated the presence of CS reactive nAAbs in the serum samples taken from three populations 1.) healthy individuals, 2.) autoimmune patients and 3.) patients who underwent hearth transplanted procedures. These nAABs were presented in elevated concentration in autoimmun patients, and belonged to the IgM isotype, while in the serum samples of hearth transplanted patients the antibodies against CS belonged to the IgG isotype. Our results show that while there is no favored region of the CS molecule recognized exclusively either by healthy individuals, autoimmun or hearth transplanted patients, the fine epitope pattern is different in the groups examined. We analyzed cross-reactive epitopes on human, bacterial CS and other mitochondrial enzymes. We have found three cross-reactive epitopes between human and bacterial CS, but there was no cross reactivity with other inner membrane enzymes (malate dehydrogenas and pyruvate dehydrogenase).

The anti-CS nAAbs by participating in the nAAb network, could function in innate defense mechanisms and at the same time recognize a target antigen in a systemic autoimmune disease. Thus, at the level of recognized epitopes there is a possible new link between the innate like component and the adaptive-autoimmune arm of the humoral immune system. nAAbs that are present in the serum of both healthy humans and patients suffering from systemic autoimmune diseases recognize a set of evolutionarily conserved self-structures. Because of their endosymbiotic evolutionary origin, proteins compartmentalized into mitochondria represent an interesting transition from prokaryotic foreign (non-self) to essential (self) molecules.

The investigation of pathological autoimmunty was performed in the experimental mouse model of the rheumatoid arthritis (rhG1-induced-arthritis (GIA)) by using two T cell transgenic mouse strain wherein the 90% of CD4+ T cells recognize the arthritogen epitope of cartilage proteoglycan-aggrecan. Thus we were able to examine the role of T cell signaling in the pathomechanism of arthritis in GIA.

We demonstrated that cell signaling through the TCR plays critical role in the induction of arthritis by the influence of balance between T cell activation and apoptosis. The „optimal" strength of T cell signaling leads to clonal expansion of autoreactive T cells and deterioration of the clinical phenotype. On the contrary, the „supraoptimal" cell signal couses the activation induced cell death of T cells, and a milder form of arthitis developes.

In conclusion, nAAB network as a key component of physiological autoimmunity plays an important role in the maintenance of the active tolerance. Any disfunction in the cell function affecting the deletion or expansion of autoreactive lymphocytes leads to pathological autoimmunity. The defective regulation of the network formed by the three levels of the immune system (innate, natural and adative) results in pathological autoimmunity.

INTRODUCTION

A key feature of the immune system is the ability to distinguish the normal self from the foreign/non-self or modified-self antigenes. While against external antigens the immune system step up with targeting immune reactions, till then self antigens are strictly tolerated. In the developement of tolerance two mechanisms play important role: i) *central tolerance* ensures that no potential autoreactive lymphocytes can leave the primary lymphoid organs ii) *peripheral tolerance* controls the possible autoimmune reactions on the periphery.

In the past few decades in several studies low affinity antibodies (of IgM istype) against genetically conserved self antigens were succesfully demonstrated in the serum of both healthy and patients with systemic autoimmune diseases. These observations supported the concept of the *immunological homunculus* (Cohen), which presumes the exist of a network formed by low affinity autoantibodies (mainly IgM) and γ/δT cells. This network reacts with genetically conserved autoantigens, and provides the defense of these self antigens from the targeting reactions of the immune system. $CD5^+$ B cells play crucial role in the developement and maintenance of this network by the production of low affinity „natural autoantibodies" (nAAb) mostly of IgM isotype. Several functions have been suggested for nAAbs: they may participate in the selection of immune repertoires, play a role in the acceleration of primary immune responses, aid the clearance of apoptotic cells, possess anti-inflammatory effects and contribute to the maintenance of immune homeostasis. These subsets of cells exhibit common phenotypic characteristics and posses both innate and adaptive features, suggesting a transitional stage in the immune system's evolution.

On the basis of these findings „***physiological autoimmunity***" is a substantive and inseparable part of the biological phenomenon called „***immunological steady-state***" (Radruch). From this aspect we can say, when the „*immunological steady-state*" splits in patients with autoimmune diseases, „pathological autoimmunity" appears and causes serios destruction of self tissues and cells by the production of autoagressive T cells and/or antibodies. In general we can say that in the developement of an autoimmune disease we should assume a change in the dinamics/homeostasis of the whole network of the immune system, rather than blaming a single factor for the appereance of the abnormal phenomena. The split of the balance after a dysfunction in the immune regulation (such as infection) can stibilize the immune homeostasis in a new equilibrium position. Since when we can speak about autoimmune disease, is determined by the fact how dominant is the autoreactive tissue destruction in that new balanced position. New environmental effects (such as another infection) can disturbe this balance and result in the further changes of the *immunological steady-state* and the progression of the disease.

Since the immunological recognition of conserved antigens –by the network of nAAbs- play a crucial role in both pathological and physiological autoimmunity, in the first part of our work we performed detailed epitope mapping of mitochondrial inner membrane enzyme (citrate-synthase, malate dehydrogenase and pyruvate dehydrogenase) specific autoantibodies by using a synthetic overlapping peptide system and phage-display technology. We succesfully demonstrated CS-specific nAAbs in the serum samples of healthy individuals, autoimmune and hearth transplanted patientes. We examined the possible homologies between the epitopes recognised by nAAbs on human and bacterial CS, and the changes of physiological autoimmunity under pathological and autoimmune conditions.

Approximately 5% to 7% of the european and north american population is affected by autoimmune dieseases. There are several experimental animal models for

the better understanding of the pathomechanisms of these autoimmune diseases. In the second part of our work we performed researches in the animal model of rheumatoid arthritis (RA) (proteoglycan/rhG1-induced arthritis in BLAB/c mice). PGIA and GIA have all the important characteristics, and clinical parameters of human RA.

RA, a systemic autoimmune disease affecting 1% of the human population, progresses from severe inflammation to deformities and loss of function of peripheral joints. Several animal models have been developed to mimic one or more characteristics of this human disease. Cartilage proteoglycan (PG)-induced arthritis (PGIA) in BALB/c mice is a T cell-dependent and B cell/antibody-mediated autoimmune disease. Several lines of evidence indicate the role of T cell involvement in the pathogenesis of PGIA.

The cartilage PG (aggrecan) molecule consists of a large core protein (>200 kDa) to which hundreds of glycosaminoglycan side chains are attached. The G1 globular domain of cartilage PG contains several dominant/ arthritogenic epitopes, whereas a few cryptic or subdominant epitopes are located in the other regions of the PG molecule. In a recent study, we replaced the fulllength PG molecule (the PGIA model) with a recombinant human G1 (rhG1) domain to immunize BALB/c mice, resulting in G1 domain-induced arthritis (the GIA model). The clinical phenotype, histopathological abnormalities and laboratory test results in the GIA model were very similar to those described in 'parental' PGIA. Because the dominant and possibly most arthritogenic '5/4E8' T cell epitope (^{70}ATEGRVRVNSAYQDK^{84}; the core sequence is underlined) is located in the G1 domain, we generated T cell receptor (TCR) transgenic (TCR-Tg) mice, in which more than 90% of the $CD4^+$ T cells expressed the Vα1·1 and Vβ4 chains recognizing the 5/4E8 epitope within the G1 domain of human PG. The first 5/4E8 epitope (PG)-specific TCR-Tg line (henceforth TCR-TgA) had been used for a number of immunological studies and adoptive transfer experiments, whereas the second transgenic line (henceforth TCR-TgB) had not yet been characterized. As both TgA and TgB strains express the same epitope (5/4E8)-specific TCR, we expected that these mice would develop arthritis similarly upon rhG1 immunization. Contrary to this, TCR-TgB mice exhibited delayed onset and less severe arthritis than TCR-TgA mice in response to either PG or rhG1 immunization, and they failed to develop spontaneous arthritis at an advanced age, whereas it is a characteristic phenotype of TCR-TgA mice. In the present study, we investigated the possible underlying mechanisms of these profound differences. Contrary to the clinical phenotype the $CD4^+$ T cells of TCR-TgB mice expressed twice as much TCR on their surface when compared to the TCR-TgA line. Our results confirm that the TCR signal in TCR-TgB mice was significantly stronger than in TCR-TgA mice, which led to extensive activation-induced cell death (AICD) of $CD4^+$ T cells attenuating the arthritic phenotype. We conclude that TCR signal strength controls the onset and severity of arthritis by regulating AICD of T cells.

OUR AIMS

Epitope mapping of mitochondrial inner membrane enzyme-specific autoantibodies- the role of natural autoantibodies in autoimmunity

1. Detection and quantification of genetically conserved mitochondrial inner membrane enzyme-specific (malate dehydrogenase (MDH), pyruvate dehydrogenase (PDH) and citrate synthase (CS)) nAAbs in the sera of healthy individuals, autoimmune and hearth transplanted patients.
2. *In silico* prediction of the possible epitopes, and the synthesis of the overlapping decapeptide system for epitope mapping of human CS specific autoantibodies.
3. Affinity purification of anti-mammalian CS nAAbs, and the determination of the isotype of the affinity purified serum samples.
4. Construction of a human CS antigen fragment library displayed on phage lambda, and the epitope mapping of affinity purified nAAb with phage-display technology.
5. Cross reactivity testing of affinity purified nAAb with other mitochondrial inner membrane enzymes, and bacterial CS.

Investigation of pathologic autoimmunity in the rhG1-induced arthritis (GIA) model

1. Comparison of the clinical phenotype (incidence and severity) of arthritis in the two TCR-Tg line.
2. Measurement of the most important serum parameters (antigen-(rhG1)-specific antibodies by enzyme-linked immunosorbent assay (ELISA) and serum cytokines by cytokine bead array (CBA)). Comparison of the result in the two strains.
3. Identification and characterization of lymphocytes participating in the induction and maintenance of arthritis based on the measurement of cell surface markers by flow cytometry.
4. Measurement of the phosphorylation of TCR signaling proteins after *in vitro* antigen stimulation with phospho-flow techniq and flow cytometry.
5. Detection of antigen induced cell death (AICD) upon antigen stimulation in the T cell cultures of the two TCR-Tg line.

METHODS

Epitope mapping of mitochondrial inner membrane-specific antibodies

1. Patients and collection of control sera

Serum samples from healthy individuals: 63 Hungarian blood donors from the Blood Transfusion Service of Baranya county, Pécs; a standardized panel from 51 British blood donors and 176 Finnish blood donors (by the courtesy of professor G. Füst and Z. Prohaszka, 3rd Department of Internal Medicine at the Semmelweis University, Budapest); 44 serum samples from healthy infants from the Pediatrics Clinic, University of Pécs, and samples of patients with systemic autoimmune diseases: 326 clinically well-documented cases of systemic lupus erythematosus (SLE), rheumatoid arthritis, undifferentiated connective tissue disease, polymyositis/dermatomyosits, systemic sclerosis, Raynaud syndrome and Sjörgen syndrome from the Immunology and Rheumatology Clinic, University of Pécs were used in this work with the permit of the Ethical Committee of the Medical Center of the University of Pécs.

2. Detection of mitochondrial enzyme specific autoantibodies by ELISA

96-well polystyrene plates (NUNC) were coated with CS, malate dehydrogenase (MDH; EC 1.1.1.37) and pyruvate dehydrogenase (PDH; EC 1.2.4.1) from porcine heart (Sigma) in 0.1M bicarbonate buffer, pH 9.6. Following the saturation of non-specific binding sites with 0.5% gelatin (Sigma) in PBS (pH 7.3), serum samples were incubated in triplicates at 1:100 dilutions in washing buffer (PBS, 0.05% Tween 20) for 60 min. Finally, the plate was incubated with HRPO conjugated anti-human-IgA, or -IgG or –IgM specific secondary antibody (Dako) for 60 min. The reaction was developed with o-phenylenediamine (Sigma), and measured on an iEMS MF microphotometer (ThermoLabsystem) at 492 nm. Cut off values of each groups examined were calculated from the average of measured OD492 data. Sera having higher OD value than average + 2SD were considered positive. All measurements were standardized with a monoclonal anti-citrate synthase antibody (Clone 4H3-E5) we produced. We used the positive serum samples for further epitope mapping of CS enzyme.

3. In silico prediction

With professional computer techniques we could predict the possible epitopes based on special molecular databases, which able to calculate (based on the structure of protein, hidrophobicity, hibrophilicity, antigenity index...) the peptide sequences that are most probably recognised by antibodies. We performed in silico prediction tests for the CS enzyme. According to the results the Peptide Chemistry Institute (MTA, Budapest) synthetised the pin-bound decapeptide system for multi-pin ELISA tests. The 10 amino acid longe synthetised fragments contained all the predicted epitopes, and followed each other with 5 amino acid overlap. Using these pin-bound decapeptides we could identified the real epitope patterns in the investigated gruops.

4. Multi-pin ELISA tests performed with synthetic pin-bound decapeptides

After the blocking of non-specific binding sites (with PBS containing 0,1 % sodium-azyde, 0,1 % Tween20 and 0,5 % gelatin, for 30 minutes), we washed 3 times the 96 well NUNC ELISA plates containing the pins. The serum samples were diluted in 1:100, and transfered on the plates in duplicates. The pins were immersed and incubated for 1 hour in the wells containing the serum samples. After washing, the diluted HRPO-conjugated secondary antibodies (IgG-1:6000 / IgM-1:1000) were pipetted on the

plates. The pins were immersed and incubated in the secondray antibodies for 1 hour. After washing we developed the reaction with ortho-phenyl-diamin (OPD), and analysed with spectrophotometry.

5. Affinity purification of sera on CS

CS from porcine heart was coupled to cyanogen-bromide activated sepharose 4B (Sigma) according to the manufacturer's instructions. Fifteen ml sera of 30 healthy blood donors and 14 patients with autoimmune disease were passed three times through the CS-sepharose resin. After washing antibodies were eluted in glycine-HCL pH 2.5, fractions were neutralized with 1 M TRIS and were tested for CS reactivity with indirect ELISA using HRPO conjugated anti-human-IgA, or -IgG or –IgM specific secondary antibody (Dako)

6. Construction of a CS antigen fragment library

Total RNA was isolated using TriReagent (Sigma) from 3x106 mononuclear cells obtained by Ficoll Paque (AmershamPharmacia) gradient centrifugation from peripheral blood of a healthy blood donor. 5 μg total RNA was reverse transcribed with Superscript II RT (Invitrogen) according to the manufacturer's instructions. cDNA encoding for the full length human mitochondrial citrate synthase was amplified with the following primers: 5'-ATGGCTTTACTTACTGCGGC-3' and 5'-TTACCCTGACTTAGAGTCCAC-3'. The PCR reaction contained 300mM of each dNTP, 1.5 mM MgSO4, 1 μM of each primer, 5 μl cDNA and 5 units of ProofStart DNA polymerase (Qiagen) in a 100 μl final volume, cycling was done with the following profile: 95 C 5min, 35 cycles of 95 C 1min, 51 C 30s, 72 C 2min, final extension at 72 C for 10 min. The PCR product was separated on a 1.5% agarose gel and purified using the Quiaquick Gel Extraction Kit (Qiagen). Following A-addition it was cloned into a T/A vector using the InsT/Aclone PCR Product Cloning Kit (Fermentas). The identity of insert was verified by sequencing on an ABI3100 Avant genetic analyzer.

Library construction was done using the lambdaD-bio phage display vector (a kind gift from Dr. Alessandra Luzzago; Instituto di Ricerche di Biologia Molecolare, Italy) as described. In brief, inserts were produced by tagged random primed elongation and amplification using SpeI and NotI tagged random primers and CS cDNA as template excised with BamHI and EcoRI (Promega) digestion from the plasmid mentioned above. Following purification with the Quiaquick PCR purification kit (Qiagen) and size selection on Wizard columns (Promega) inserts were digested with SpeI and NotI (Promega). Twenty ligations were set up containing 1 μg of SpeI/NotI digested lambdaD-bio DNA, 25 ng of SpeI/NotI digested insert, 30U of T4 DNA ligase (Fermentas) in a final volume of 5μl and incubated 48 hours at 4C . The ligation mixture was phenol-chloroform extracted, ethanol precipitated and packaged with the Ready To Go Lambda Packaging Kit (AmershamPharmacia). Phage were amplified by infecting log phase E.coli BB4 cells and plating them on LB agar plates. After plaque formation phage were eluted by an overnight incubation in SM buffer (100mM NaCl, 8.1 mM MgSO4, 50mM Tris-HCl pH 7.5), concentrated with polyethylene glycol precipitation and resuspended in SM buffer supplemented with Complete EDTA Free Proteasae Inhibitor Cocktail (Roche).

7. Affinity selection of CS antigen fragment library

Affinity selection of CS antigen fragment library with CS affinity purified sera was performed essentially as described. Briefly, microtiter plates were coated with affinity

purified anti-CS sera or anti-CS mAb 4H3E5 (developed in our lab) at 10 μg/ml in coating buffer. After blocking 10^{10} phage were incubated for 2 h at room temperature. Wells were washed five times and bound phages were recovered by in well infection of E.coli BB4 cells. The infected bacteria were plated on LB agar plates and phage were eluted then concentrated as described above. The affinity selection was repeated one more time and individual clones were picked up for DNA sequencing.

8. Cross reactivity testing of CS affinity purified sera

Cross reactivity with additional mitochondrial inner membrane enzymes was tested with indirect ELISA using MDH and PDH from porcine heart (Sigma) as antigens.
Reactivity with E.coli CS was tested with pin-bound overlapping decapeptides as described previously.

The rhG1-INDUCED ARTHRITIS MODEL

1. Animals

We used two lines (Tg 'A' and Tg 'B') of the TCR-Tg mice, both expressing the TCR Va1·1 and Vb4 chains specific for the major dominant arthritogenic '5/4E8' epitope (ATEGRVRVNSAYQDK) of the G1 domain of human cartilage PG. The two transgenic (TCR-TgA and TCR-TgB) lines were generated from different pronuclear injections using the same construct. Transgene-positive founders were backcrossed 12 times into the BALB/c (Charles River Laboratory, Kingston Colony, NY, USA) background. All animal procedures were conducted according to the protocol approved by the Institutional Animal Care and Use Committee at Rush University Medical Center (Chicago, IL, USA).

2. Antigens, immunization, clinical assessment of arthritis and sample collection

Recombinant human G1-domain (rhG1) was purified as described. Wild-type (WT) BALB/c mice (Charles River) and age-matched 3-month-old female transgenic (TCR-TgA and TCR-TgB) mice were immunized intraperitoneally with 20 mg rhG1 in an emulsion of 2mg dimethyldioctadecylammonium bromide adjuvant (in 100 ml of PBS) on days 0, 21 and 42. The mice were examined three to four times a week after the second immunization for the clinical assessment of arthritis. The onset time and incidence of arthritis were recorded, and disease severity was scored visually based on the degree of swelling and redness of each paw, ranging from 0 to 4, yielding a maximum severity score of 16 per mouse. From each transgenic line and WT BALB/c mice, four animals were killed at different time-points: before immunization (naive mice), 10 days after the first immunization, 4 days before the second and third immunizations and 5 days after the second and third immunizations. These six timepoints were determined in preliminary experiments. Blood samples, joint-draining lymph nodes [brachial, axillary, inguinal and popliteal lymph nodes (LNs)] and spleens were collected for flow cytometry analysis and cell culture. Serum samples were collected for measurements of antibody and cytokine concentrations.

3. Measurement of antigen (rhG1)-specific antibodies by enzyme-linked immunosorbent assay (ELISA) and serum cytokines by cytokine bead array (CBA)

Serum anti-rhG1 IgG1 and IgG2a antibodies quantified by ELISA using serially diluted serum samples. Purified recombinant human G1 without the Fc tail, was immobilized in Maxisorp 96-well plates (Nunc International) at a concentration of 0.1 μg/well each. For rhG1-specific IgG isotype assays, peroxidase-labeled goat antimouse IgG1 antibody

(Zymed) or IgG2a (BD Biosciences) was used after incubation with serum. Serum PG-specific antibody levels were calculated using serial dilutions of pooled sera of mice with PGIA and known antibody titers. Serum interleukin (IL)-1b, IL-4, IL-6, tumour necrosis factor (TNF)-a, IL-17A, IL-12p70 and interferon (IFN)-g were measured using the CBA mouse/rat soluble protein flex set assay (BD Biosciences, San Jose, CA, USA), according to the manufacturer's instructions. The samples were measured using a BD fluorescence activated cell sorter (FACS)Canto II flow cytometer equipped with a High Throughput Sampler (HTS) module (BD Biosciences); 500 events (measured twice) per analysis were recorded. Data were analysed using FCAPArray software (Soft Flow Hungary Ltd, Pécs, Hungary).

4. Flow cytometry

Cell surface markers of peripheral blood, LN and spleen leukocytes were analysed by multi-colour flow cytometry. Data acquisition and analysis was performed using a FACS Canto II flow cytometer with an HTS module and FACS DIVA software (BD Biosciences). Initial gating was performed on lymphoid cells based on the forward-/sidescatter (FSC/SSC) parameters.The following cell populations were defined based on the cell surfacemarkers: B220+: total B cells; CD3+: total T cells; CD3+/CD4+: CD4+ T cells; CD3+/ CD8+: CD8+ T cells; CD3+/CD4+/CD25high: activated T cells; CD3+/CD4+/CD44high: activated (memory) T cells.

5. Cell separation, culture condition and in vitro antigen stimulation

T cells were purified from the spleens of TCR-Tg mice using an EasySep magnetic T cell enrichment kit (Stem Cell Technologies, Vancouver, BC, Canada). The purified T cells ($8x10^5$) were seeded onto irradiated A20 (BALB/c B cell lymphoma) antigen presenting cells (ATCC, Rockville, MD, USA) that can present the 5/4E8 peptide. A20 cells ($1x10^5$ cells/well) were plated in 48-well plates, precultured with or without the synthetic 5/4E8 peptide (5 μg/ml) for 12 h and then washed with serum-free DMEM. For apoptosis studies, purified T cells from spleen were co-cultured with these pretreated and washed A20 cells in 600 μl of DMEM containing 10% fetal bovine serum for 3 days. For signaling studies, $3x10^5$ purified T cells from spleen were spun onto a layer of pretreated A20 cells by short centrifugation (900*xg*, 3 min) and harvested after 1 h of co-culture.

6. Saturation binding test

CD4+ T cells were separated from the spleens of TCR-TgA and TCR-TgB mice by magnetic enrichment. Exactly the same number of cells from each line was stained with increasing concentrations of fluorescently labelled anti-TCR Vβ4, anti-CD3 or anti-CD4 mAbs, and binding was analysed by flow cytometry. The mean fluorescence intensity (MFI) values were corrected by subtracting the MFI values of isotype controls, and the binding curves were fitted to the titration data points using GraphPad Prism 4·0 (GraphPad, San Diego, CA, USA).

7. Detection of TCR Va1•1 and Vb4 chain genomic copy numbers by real-time quantitative polymerase chain reaction (qPCR)

Tail genomic DNA was isolated from homozygous TCR-TgA and TCR-TgB animals by proteinase K digestion followed by phenol–chloroform extraction. Extracted genomic DNA samples were ethanol-precipitated and resuspended in Trisethylenediamine tretraacetic Acid (EDTA) buffer. The DNA samples were fragmented by restriction

endonuclease digestion with enzymes cutting outside the PCR-investigated regions. Digested DNA was purified using a Qiaquick kit (Qiagen, Carlsbad, CA, USA), and DNA concentration was determined photometrically; qPCR was performed in triplicate with 10, 5, 2·5 and 1·25 ng of input DNA using SsoFast™ Probes Supermix (Bio-Rad). PrimeTime™ qPCR primers and dual-labelled probes (IDT, Coralville, IA, USA) were applied to determine the copy numbers of TCR alpha and beta chains (sequences of PCR primers and dual-labelled probes are available upon request); qPCR was performed using an iQ5 instrument (Bio-Rad, Hercules, CA, USA). For normalization, we used the promoter region of the TATA-box binding protein (TBP) gene as a single-copy control.

8. Apoptosis detection by annexin V/7-AAD staining

Annexin V/7-AAD staining was used to distinguish between early and late apoptotic T cells. Labelling was performed according to the manufacturer's (BD Biosciences) instructions. The cells were analysed by flow cytometry immediately. Annexin V-/7-AAD- cells were considered nonapoptotic. Annexin V+/7-AAD- cells were considered early apoptotic, and annexin V+/7-AAD+ cells were considered late apoptotic.

9. Determination of phosphorylation of TCR signaling

Phosphorylation of zeta-chain-associated protein kinase 70 (ZAP-70), extracellular regulated kinase1/2 (ERK) and p38 was detected using the phospho-flow technique according to the manufacturer's instructions using phosphorylated protein-specific mAbs (BD Biosciences). After *in vitro* TCR stimulation, cells were labelled with anti-CD4-PerCPCy5·5 and phospho-specific antibodies: PE-conjugated anti-mouse pZAP-70 (clone 17A/P-ZAP-70) recognizing pY319 of ZAP-70, PE-conjugated anti-mouse pERK1/2 (clone 20A) recognizing pT203/pY205 in ERK1 and pT183/ pY185 in ERK2, and PE-conjugated anti-mouse (clone 36/p38 (pT180/pY182) recognizing pT180/pY182 in p38.

10. Statistical analysis

Descriptive statistics was used to determine group means and the standard errors of the means (the mean $\pm$ s.e.m.). Differences between two groups were tested for statistical significance using Student's t-test and differences among three or more groups were tested by analysis of variance (anova) with Dunnett's post-hoc t-test. A value of $P \leq 0{\cdot}05$ was considered statistically significant.

RESULTS

Epitope mapping of mitochondrial enzyme-specific antibodies

1. Anti-mitochondrial enzyme specific antibodies in healthy individuals, systemic autoimmune and hearth transplanted patients

Using simple binding ELISA we demonstrated the presence of antibodies recognizing CS, MDH, and PDC in the sera of each groups. Isotype-specific ELISA showed that enzyme-specific antibodies with IgM isotype are more frequently present in all investigated groups than those of IgG or IgA isotypes. No differences were found among the subgroups of healthy individuals; however, the incidence of anti-CS and anti-MDH autoantibodies with IgM isotype was significantly higher in autoimmune patients compared to the healthy controls.

We continued our investigations with CS specific IgM autoantibodies, as this group showed the most characteristic pattern of distribution. We followed the titer of anti-CS IgM antibodies, with repeated sample collection minimum 3 times over a 5 years period. We found that the CS reactivity of individual sera remained permanently constant over this period. Our findings that the majority of these antibodies have IgM isotype, are already present in infants, and the long term stability of their serum titers in adults indicate that these specificities belong to the nAAb repertoire established early in postnatal life.
We screened sera of heart transplant patients for anti-CS antibodies. The appearance of anti-CS IgG could be the result of adaptive immune response triggered by either foreign antigens or release of CS into the circulation from internal organs as heart and liver during pathological conditions. We sought that CS is released during post-transplantation vasculopathy, and this could elicit an adaptive type immune response. Indeed we have found that the frequency of high titer anti-CS IgG in sera of heart transplant patients is significantly higher than in healthy individuals (20% vs. 4%). The presence of induced anti-CS IgG in heart transplant patients raise the question whether these antibodies are produced as a result of isotype switch from nAbs with IgM isotype or produced against different epitopes originally not recognized by nAbs. Epitope mapping of anti-CS IgGs suggested an altered epitope pattern compared to healthy individuals.

2. Epitope mapping of antibodies against human citrate synthase with the use of overlapping synthetic decapeptides

We performed detailed epitope mapping analysis of anti-CS antibodies with the use of overlapping synthetic decapeptides. We have shown that, while there is no favored region of the hCS molecule recognized exclusively either by healthy individuals or patients with autoimmun disease, or hearth transplanted patients, the fine epitope pattern is different in the three groups examined.

3. Epitope mapping of antibodies against bacterial citrate synthase with the use of overlapping synthetic decapeptides

Since a number of studies demonstrated that nAAbs play an important role in first line defense mechanisms of the humoral immune response, we analyzed the possible overlap in epitopes recognized on hCS and bCS. On the basis of comparative epitope mapping with sera from healthy individuals, patients with systemic autoimmune diseases and heart transplant patients epitopes recognized on bCS could be grouped into the following categories: epitopes recognized by sera of all individuals, epitopes recognized only by sera of healthy individuals, and epitopes recognized only by sera of patients with systemic autoimmune diseases and heart transplant patients. There were no differences in the epitope pattern among autoimmune patients and heart transplant patients.

4. Affinity purification of CS reactive sera

To exclude the masking effects of nonspecific bindings we purified anti-CS antibodies from 44 human sera (30 healthy and 14 autoimmune patients: 9 with SLE, 3 with systemic sclerosis and 2 with rheumatoid arthritis) by affinity chromatography for further experiments. Affinity purification was successful only in those cases (2 healthy and 2 SLE patients) where the actual serum had extraordinary high (OD492 >1.5) anti-CS reactivity. The eluted anti-CS antibodies from such sera were exclusively with IgM isotypes.

5. Epitope mapping of affinity purified antibodies against hCS with the use of hCS antigen fragment library displayed on phage lambda

We proceeded to the epitope mapping of affinity-purified anti-CS sera. Following two rounds of affinity selection 20 clones selected with each serum were picked up for DNA sequencing. In contrast to the selection with our anti-CS mAb, these clones carry short peptide sequences which could also be aligned to human CS. These short sequences are scattered throughout the human CS sequence and it seems that practically the same regions of the molecule are recognized by the two groups of sera. According to our results obtained with phage displayed antigen fragments, while there is no favored region of the CS molecule recognized exclusively either by healthy individuals or patients with SLE, the fine epitope pattern is different in the two groups examined.

6. Cross reactivity testing of CS reactive sera

Cross-reactivity of the affinity purified anti-CS antibodies with other mitochondrial inner membrane enzymes (MDH and PDC) was tested by indirect ELISA. The affinity-purified anti-CS antibodies did not recognize any of these antigens.

We investigated the possible overlap in nAAb recognized epitopes on mammalian and bacterial CS. Due to the prokaryotic origin of mitochondria, CS represents an attractive target molecule to examine the self-reactive nAAbs' capability to recognize epitopes on the foreign counterpart of the same molecule. To achieve this, we used sera affinity purified on mammalian CS for epitope mapping on CS from E.coli, using the overlapping synthetic peptide method. Only three cross reacting sequences were found: amino acids 124-133: FRRDSHPMAV (identity with human CS: 40%, similarity: 60%); amino acids 174-183: MCYKYSIGQP (identity with human CS: 30%, similarity: 40%) and amino acids 351-360: YFIEKKLYPN (identity with human CS: 40%, similarity: 60%), respectively. The three recognized sequences show only a limited homology with human CS, even though identical amino acids with a possible anchor function are present at corresponding positions. These amino acids contain either polar or charged side chains, which is in agreement with previous reports about the preferential amino acid composition of nAAb epitopes. The three peptides, according to the three dimensional model, are located on the surface of the molecule. Moreover, two of the peptides (124-133 and 174-183), though separated by 50 amino acids in the primary sequence, are in close proximity on the structural model of folded protein, indicating that they represent the same antigenic region.

The rhG1-induced arthritis model

1. Onset and severity of arthritis differ in the two PG-specific TCR-Tg lines

Previous studies have shown that mice of the original (first) 5/4E8 PG epitope-specific TCR-Tg (TCR-TgA) mice are highly susceptible to PGIA. After finishing the backcross of the second 5/4E8 PG epitope-specific TCR-Tg strain (TCR-TgB) into BALB/c background we immunized the two TCR-Tg strains side by side with rhG1. The TCR-TgA line responded to rhG1 immunizations as expected: arthritis had already developed a few days after the second immunization, and reached maximal severity scores with 100% incidence within 2 weeks after the second immunization. Surprisingly, the clinical phenotype and disease characteristics TCR-TgB were more similar to those found in WT BALB/c mice: the onset was delayed and the arthritis was less severe when compared to TCR-TgA mice. These results were surprising, because approximately the same proportion (~90 to 94%) of CD4+ T cells in both lines expressed the TCR Vb4 chain.

2. Immune responses against rhG1 in the two TCR-Tg strains

To determine whether the differences in clinical phenotype were associated with differences in serum parameters, we assessed the serum levels of antibodies and cytokines using antigen-specific ELISA and CBA, respectively. Anti-G1 domain-specific antibodies were hardly detectable before the second immunization in either transgenic line. The second immunization (day 21) induced significant anti-G1 IgG1 antibody secretion in TCR-TgA mice, whereas the level of this antibody isotype remained almost undetectable in TCR-TgB mice. TCR-TgA mice also exhibited higher serum levels of anti-G1 IgG2a antibodies compared to TCRTgB mice. While the relatively high deviations and relatively low animal number did not allow us to perform a correct statistical analysis during the entire immunization period, we had a sufficient number of animals in all three genotypes at the end of the experiment, showing significant differences in anti-G1 antibodies between TCR-TGA and TCR-TgB mice. This significantly higher antibody secretion observed in TCR-TgA mice was associated with a significantly higher B cell percentage compared to that in TCR-TgB mice during the whole immunization period. No significant differences were observed in the serum levels of IL-1b, IL-12p70 or IL-17 between the two TCR-Tg lines. Serum IL-6 concentration was elevated in TCR-TgA mice throughout the entire experiment. TCR-TgA mice also showed higher serum levels of IFN-□ and TNF-α, when the first symptoms (acute phase) of arthritis appeared, and compared to serum levels of these two cytokines in the TCR-TgB line.

3. Comparison of T cell activation markers, co-stimulatory molecules and the proportion of regulatory T cells in TCR-TgA and TCR-TgB mice during the course of immunization

We compared the expression of activation markers on the cell surface of $CD4^+$ T cells in the peripheral LNs and spleen to clarify whether there was any difference in the activation level of T cells in the two TCR-Tg lines. We detected a rapidly accumulating $CD25^{high}CD4^+$ T cell population after the first rhG1 injection, and the size of this cell population remained large in the peripheral LNs and spleens of TCR-TgA mice. In contrast, the ratio of $CD25^{high}CD4^+$ T cell population in TCR-TgB mice immunized with rhG1 remained as small as in naive mice during the entire experiment. The expression of the CD44 molecule (a marker of activated/memory T cells) in the CD4+ T cell population showed a similar pattern to that of CD25 in TCR-TgA mice, but was less consistent and remained significantly lower in TCR-TgB at almost all time-points tested. Because co-stimulatory molecules profoundly influence T cell activation and signaling, we examined CD28, CTLA-4, ICOS and PD-1 expression in CD4+ T cells in both TCR-Tg mouse lines. No significant differences were observed in $CD28^{high}$, CTLA-4^{high} or PD-1^{high} $CD4^+$ T cell percentages. Naive TCR-TgB mice exhibited three to four times more $ICOS^{high}CD4^+$ T cells compared to naive TCR-TgA mice. However, during immunization the proportion of $ICOS^{high}CD4^+$ T cells showed a constantly increasing trend in TCR-TgA mice, especially in the peripheral LNs. In contrast, the percentage of $ICOS^{high}CD4^+$ cells in TCR-TgB mice decreased to a very low level after the first rhG1 injection and remained at this significantly reduced level atmost time points tested. Interestingly, a peak of both CD44 in LNs and ICOS in spleen expression was observed in $CD4^+$ T cells in TCR-TgB mice 5 days after the second rhG1 injection, which may indicate a temporary (short-term) activation of these preactivated $CD4^+$ T cells following the antigen injection.

Tregs play an important role in regulating immune functions by limiting the activation of T and B cells. Their impaired function or reduced numbers may lead to

autoimmunity. Therefore, we hypothesized that the reduced arthritis susceptibility in TCR-TgB mice may be due to a significantly higher level of Tregs that could suppress autoreactive T cells. We compared the Treg ratios in naive transgenic mice, but no significant difference was found between TCR-TgA and TCR-TgB mice. Unexpectedly, in response to immunization, a considerable Treg expansion was observed in TCR-TgA mice, especially in the peripheral LNs, which was not found in TCR-TgB mice. Although there was an upregulation of Tregs in the spleens of TCR-TgB mice after the 2nd and 3rd immunizations, significantly more Tregs were found in the spleens of TCR-TgA mice during the entire experiment.

4. Accelerated in vitro apoptosis in TCR-TgB CD4$^+$ T cells

Impaired AICD of arthritogenic T cells is considered to be one of the underlying mechanisms in the development of arthritis, and we have observed previously spontaneous arthritis in aging TCR-TgA mice. Therefore, we hypothesized that the phenotypic differences between the two lines might be attributed to differences in T cell signaling and apoptosis. Accelerated apoptosis of CD4$^+$ T cells in TCR-TgB mice could explain the phenotype of attenuated arthritis. Therefore, we cultured purified CD4$^+$ T cells with 5/4E8 peptide pretreated irradiated A20 antigenpresenting cells for 3 days in vitro and measured the antigen stimulation-induced apoptotic T cell death. The percentage of early apoptotic (annexin V$^+$/7-AAD$^-$) T cells was significantly higher in the cell cultures harvested from TCR-TgB mice during the entire immunization period, whereas the corresponding CD4$^+$ T cell cultures of TCR-TgA mice contained significantly more viable (non-apoptotic annexin V$^-$/7-AAD$^-$) T cells.

5. Higher TCR expression and TCR signaling strength in CD4+ T cells in TCR-TgB compared to TCR-TgA mice

AICD is controlled by TCR signal strength together with co-stimulatory signals. Although the two transgenic lines expressed TCRs specific for the same epitope (same transgenic construct), they were generated independently. Therefore, it was possible that the TCR expression on CD4$^+$ T cells from the two transgenic lines was different.We compared the cell surface expression of TCR Vβ4, CD3 and CD4 in transgenic T cells using a flow cytometric saturation binding test. Surprisingly, TCR-TgB mice expressed approximately twice as much TCR Vβ4 and CD3 as TCR-TgA mice, but the amount of CD4 was similar in both strains. Thus, the amount of CD4 expression did not correlate with other components of the TCR complex such as Vβ4 and CD3. To confirm this difference, we determined the copy numbers of the TCR-Tg Vβ4 and Vα1·1 chains by qPCR in the genomic DNA isolated from both TCR-Tg lines. Interestingly, there were seven copies of Vα1·1 but only three copies of Vβ4 of the transgene in homozygous TCR-TgA mice, whereas there were six copies of both TCR chains in homozygous TCR-TgB animals. Because TCR is always expressed as a heterodimer on the surface of peripheral T cells, these qPCR results confirmed the results of our flow cytometric analysis, demonstrating that TCR-TgA mice indeed expressed half as much TCR as TCR-TgB mice. The higher TCR expression, associated with the delayed onset and decreased severity of arthritis, prompted us to determine if AICD of CD4$^+$ T cells increased in TCR-TgB mice. More specifically, we asked whether the significantly higher expression of TCR and CD3 in TCR-TgB mice correlated with the phosphorylation levels of ZAP-70, ERK1/2 and p38, three key parameters of T cell signal strength. To this end, purified CD4$^+$ T cells were co-cultured with A20 cells in the presence of the 5/4E8 peptide for 1 h.We found that the TCR signal-elicited

phosphorylation of ZAP-70 and p38 was significantly higher in TCR-TgB than in TCR-TgA mice, whereas ERK1/2 phosphorylation was similar.

DISCUSSION

Epitope mapping of mitochondrial inner membrane enzyme-specific autoantibodies- the role of natural autoantibodies in autoimmunity

As genetically conserved antigens play a special role in both physiological and pathological autoimmunity, we used mitochondrial inner membrane enzymes as model antigens for the demostration of nAAbs in the serum samples of helthy blood donors, autoimmune and hearth transplanted patients by immune serological methods. Low affinity autoantibodies from IgM isotype (in low concentration) were present in all three investigated groups. The amount of these antibodies were stabel, and the individual values did not change in time. Autoantibodies with high serum concentrations from IgM isotype were significantly more frequent in the patients with autoimmune conditions, while antibodies with elevated serum concentration from IgG isotype were specific for heart transplanted patients. We sought that CS is released during post-transplantation vasculopathy, and this could elicit an adaptive type immune response. The presence of autoantibodies with IgG isotype could be the result of the targeting type immune responses against the foreign transplanted graft. In autoimmune patients the target of the pathological immune reactions is not that antigen, so it was not a coincidence when the autoantibody profile of autoimmune patients was similar to healthy individuals. The amount of autoantibodies with IgG isotype fluctuated during the years.

We presume – in accordance with the literature- that the autoantibodies with IgM isotype are part of the physiological immunity, while autoantibodies with IgG isotype take part in the pathological immune responses. We continued our investigations with the epitope mapping of these autoantibodies with the use of CS antigen fragment library displayed on phage lambda, and a synthetic overlapping decapeptide system. Our results showed that hCS-specific antibodies are present in the human sera, but we could not identified privileged regions on the enzyme typical for only one group. The fine epitope pattern on CS is different under physiological and pathological conditions. Anti-hCS antibodies with IgM isotype seem to belong to the pool of naturally occurring antibodies. Sera affinity purified on CS cross reacts with bacterial CS. Despite the fact that E.coli CS and mammalian CS exhibit long homologies in their primary structure, the cross-reactive epitopes which we identified by autoantibodies carry altered primary structures with strong identical motifs in electric charge and hydrophobicity. The epitope pattern recognized on the bCS showed more differences between the three groups when compared to the hCS enzyme.

In theory, naturally occurring antibodies “specific” for a given self antigen could fulfill the function of participating in innate defense mechanisms and at the same time recognize a target antigen in a systemic autoimmune disease. Similarly to the initiation of immune response the maintenance of tolerance involves all three compartments of the immune system. Disturbances in co-operation among innate, natural, and adaptive immune system components may result in the impairment of both targeting type immune response and the self tolerance, thus paving the way for development of immunodeficiencies and pathological autoimmune phenomena.

Investigation of pathological autoimmunity in the rhG1-induced arthritis model

Co-operation between autoreactive (Th1 and Th17) CD4+ T cells and antibody-secreting (and antigen-presenting) B cells is indispensable for the initiation and progression of systemic autoimmune arthritis. Both PGIA and GIA, similar to RA, are T cell-dependent B cell-mediated autoimmune diseases. Adoptive transfer experiments have proved that neither T nor B cells alone were sufficient for the transfer of the disease, and that only co-injection of both cell types was successful. Therefore, T–B cell co-operation is definitely required for the development of PGIA and GIA. In this TCR-Tg study we used the GIA model by immunizing mice with rhG1 protein, and stimulating/activating CD4+ T cells of TCR-Tg mice with their 5/4E8 epitope-specific synthetic peptide. We observed that rhG1 provoked severe arthritis in TCR-TgA mice, whereas a milder form of the disease with significantly delayed onset developed in TCRTgB mice, which was comparable to that described in WT BALB/c mice. This was an unexpected result, because both TCR-TgA and TCR-TgB mice possess the same 5/4E8 (PG)-specific (monoclonal) TCR expressing $CD4^+$ T cell repertoire. From the laboratory parameters analysed, elevated levels of serum anti-G1 antibodies (IgG1/IgG2a, cross-reactive with the G1 domain of mouse PG) in the TCR-TgA line, shortly after the second immunization but before the appearance of visible inflammatory symptoms, suggest that these antibodies may have contributed to the accelerated disease development. The higher B cell percentage in TCR-TgA mice was consistent with the higher serum anti-G1 antibody levels. Previous studies have indicated that the concentrations of antigen-specific antibodies in sera, especially autoantibodies, correlate well with the severity of the disease in WT BALB/c mice, and that such antibodies can already be detected long before the appearance of the first inflammatory symptoms. However, despite the higher B cell numbers at most time-points tested during the immunization period, the serum antibody levels in TCR-TgA mice never reached the levels measured in WT BALB/c controls. One possible explanation for the lower autoantibody concentration in TCR-Tg mice is the highly restricted TCR repertoire, specific for only one epitope. None the less, the role of B cells in the development of the disease is unquestionable, even in this epitope-restricted TCR-Tg model. Secretion of antigen-specific antibodies, however, is only part of B cell function because B cells are important antigenpresenting cells in PGIA and most probably in GIA as well. Therefore, specific co-operation between antigen-primed T cells and antigen-specific B cells appears to be a critical component of arthritis induction. The higher number of B cells in TCR-TgA mice could present the antigen to T cells more effectively, leading to accelerated T cell activation. Indeed, the highest expression of the T cell activation markers during the immunization with rhG1 protein was observed on TCR-TgA $CD4^+$ T cells. As mentioned above, the $CD4^+$ T cells of TCR-TgA mice, unlike those of TCR-TgB mice, expressed more activation markers, such as CD25 and CD44. Activation of $CD4^+$ T cells is central for the initiation of both PGIA and GIA, and these T cells in TCR-TgB mice were not activated as strongly as TCR-TgA T cells by immunization. Therefore, the lower percentage of activated T cells in TCR-TgB mice could account for the delayed disease onset and less severe arthritis. An additional difference between the TCR-Tg lines was that a larger percentage of $ICOS^{high}$ $CD4^+$ T cells were present in TCR-TgA mice, especially in the peripheral LNs. ICOS has been shown to be indispensable in collageninduced arthritis and K/BxN arthritis models, and certain ICOS polymorphisms are associated with RA. ICOS is expressed prominently by follicular T helper (Tfh) cells in lymphoid organs. Tfh cells have been shown to provide critical support to autoreactive B cells in systemic autoimmunity and in the initiation of arthritis

in K/BxN mice. Therefore, here, the lower percentage of $ICOS^{high}$ $CD4^+$ T cells (most probably Tfh) cells could also contribute to the diminished antibody production and the lower severity of autoimmune arthritis in TCR-TgB mice.

Tregs play a central role in peripheral tolerance and the prevention of autoimmunity, but the role of natural Tregs is controversial both in human RA and in its corresponding animal models. In the present study, an attractive explanation could have been that the higher number of Tregs were responsible for the lower incidence and diminished severity of GIA in TCR-TgB mice. On the contrary, indicating that Tregs play a dispensable role in regulating the autoimmune processes in PGIA and GIA. However, the role of Tregs in autoimmune processes, especially in arthritis, is still not completely understood, and further studies are needed to improve our understanding of the role of Tregs in RA.

The most interesting observation in TCR-TgA and TCR-TgB mice was the differential susceptibility of their $CD4^+$ T cells to activation-induced apoptosis. Upon stimulation with the 5/4E8 peptide, T cells isolated from TCR-TgB mice exhibited higher sensitivity to apoptosis compared to the $CD4^+$ T cells from TCR-TgA mice. Altered T cell apoptosis has been found to be a critical factor in the development of autoimmune arthritis, and TCR signaling threshold and co-stimulatory signals have been shown to regulate AICD. In our case, a saturation-binding test and qPCR analysis proved that $CD4^+$ T cells from TCR-TgB mice expressed twice as much TCR and CD3 molecules than the T cells from the TCR-TgA line. Variance in the number of expressed TCRs on the cell surface may significantly influence signal strength through the TCR-initiated signaling pathway. Indeed, when TCR-TgB $CD4^+$ T cells were engaged with the 5/4E8 peptide, significantly higher levels of phosphorylation of the key downstream signaling molecules (ZAP-70 and p38) were detected than in TCR-TgA T cells. In other words, the higher the TCR expression, the stronger the signaling response to the 5/4E8 epitope became. Thus, a ‘too strong’ TCR signal could have led to extensive apoptosis of self-reactive T cells during immunization with an antigen (rhG1) containing the 5/4E8 epitope. The importance of TCR signal strength has also been underlined in a recent human study: RA patients showed altered ERK and ZAP-70 phosphorylation levels upon CD3/CD28 stimulation, implicating a potential human relevance for our results.

Based on these results, we propose that TCR signal strength controls arthritis susceptibility in the two lines of PG-specific TCR-Tg mice. The differences in the phosphorylation levels of the downstream effectors in TCR signaling offered a logical explanation for the differences in arthritis severity. The different TCR levels in the two transgenic lines resulted in significant alterations of TCR signal strength. A strong PG (5/4E8 epitope)-specific TCR-initiated signal in TCR-TgA mice led to optimal T cell activation and, compared to WT, generated a ‘super-arthritic’ phenotype. In contrast, an extremely ‘strong’ TCR signal, due probably to higher TCR expression, led to in vivo T cell apoptosis and diminished arthritis in TCR-TgB mice. Thus, the correlation between TCR signal strength and arthritis severity is not linear: a weaker signal (as seen in the TCR-TgA mice) appears to be more ‘optimal’ for the activation of self-reactive T cells.

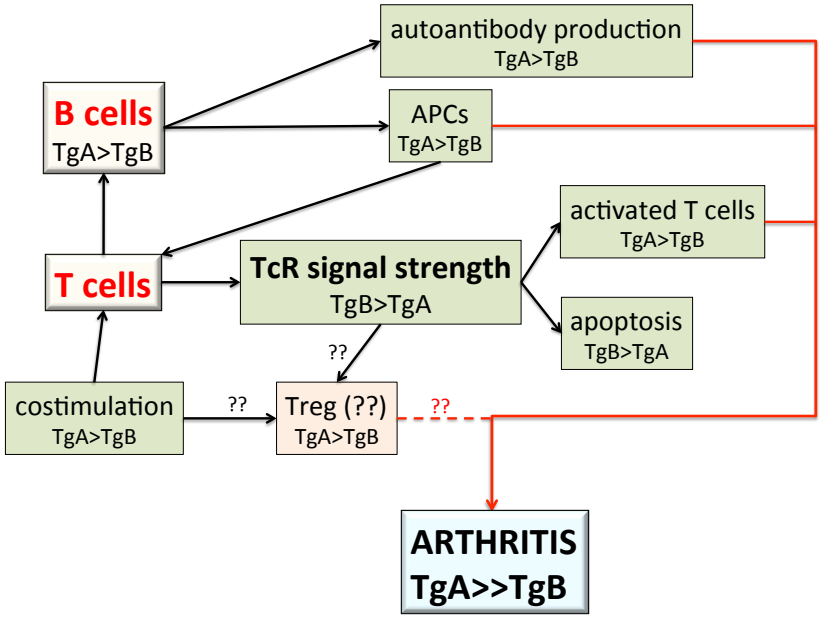

Figure 1. T cell receptor (TCR) signal strength controls arthritis severity in proteoglycan-specific TCR transgenic mice.

On the base of our results, it seems that „the immunological steady-state" is one inevitable part of the physiological immune regulation, and one way of its manifestation is the nAAb network, which reacts for example with genetically conserved mitochondrial inner membrane enzymes, like CS, and that way helps in the developement and maintenance of the tolerance against these autoantigens (Figure 2.). For the better understanding and research of the humoral autoimmunity, the detection of the regular antigen-specific antibody titers are not enough, and the analysis of the fine epitope pattern becomes necessary. The immunological steady-state, due to the network like co-operation of the whole immune system, can change in several ways and result in pathological autoimmune conditions (Figure 2.) An example is a single change in the cell function, like the alteration of the activation induced cell death of $CD4^+$ T cells in the animal model of rheumathoid arthritis which caused pathological autoimmunity and permanent serious tissue destructions. These results reveal the possible necessarity of the examination of cellular mechanisms besides the usual autoantibody screening test in the diagnostics of autoimmune diseases. Besides the cellular and humoral mechanisms of autoimmune processes the role of the genetic and environmental factors are inevitable. In conclusion, the examination and understanding of autoimmunity and autoimmune diseases needs a complex approach.

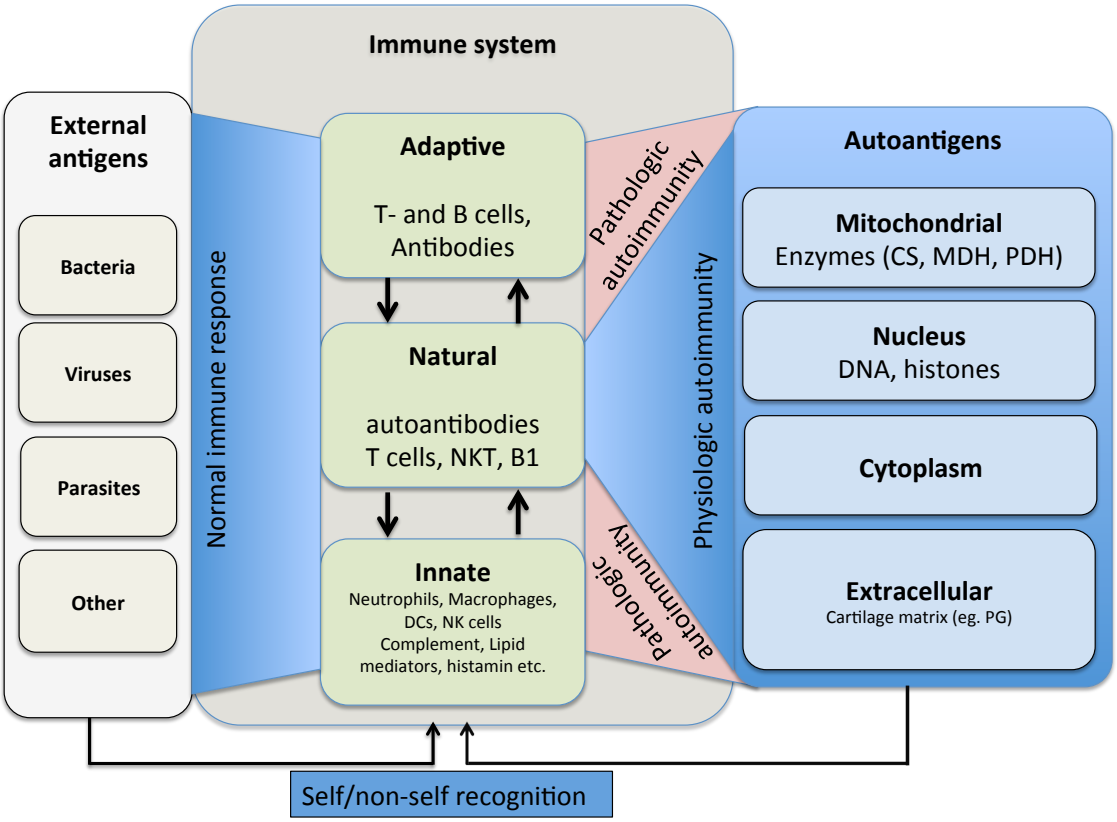

Figure 2. **Changes in the immune regulation are responsible for pathological autoimmunity.** Normal immune regulation guarantees the proper distinction between self nad non-self structures. The incoming signals are processed by different levels of the immune system. The three levels (innate, natural and adaptive) are strictly related to each other. That way the effector mechanisms decide to offend the non-self and tolerate the self antigens. The natural immune system plays an important role in the maintenance of the tolerance against autoantigens. In case of the disfunction of immune regulation the immune responses „spread „ against self antigens, and the effector mechanisms of the adaptive and innate immune systems step in, and the loss of tolerance leads to pathological auoimmunity. Physiological autoimmune mehanisms are marked with blue, and pathological autoimmunity is marked with pink color.

SUMMARY OF OUR MOST IMPORTANT NEW RESULT

Epitope mapping of mitochondrial inner membrane enzyme-specific autoantibodies- the role of natural autoantibodies in autoimmunity

1. We succesfully demonstrated the presence of mitochondrial inner membrane enzyme (CS, MDH, PDH) specific autoantibodies in all of the investigated groups (healthy, autoimmune and hearth transplanted). The subgroups of helthy individuals did not show differences in the concentration and isotype of these autoantibodies. In the serum samples of patients with autoimmune diseases the autoantibodies with IgM isotype were presented in elevated concentration, while the autoantibodies from IgG isotype with high concentration were specific for the hearth transplanted patients..
2. After in silico prediction of possible B and T cell epitopes, we constructed and succesfully used synthetic overlapping peptide system for the epitope mapping of human and bacterial CS enzyme. We could not detect dominant epitopes specific for only one investigated group. We found differences in the fine pattern of the epitops..
3. We affinty purified CS-specific antibodies from healthy and autoimmune serum samples with high CS reactivity.with the use of porcine CS. These antibodies exclusively belonged to the IgM isotype.
4. We constructed a hCS random peptide fragment library displayed on phage lambda, and performed further epitope mapping with the CS affinity purified sera. We could not detect dominant and unique epitopes with this method also.
5. Affinity purified serum samples did not show cross reactivity with other mitochondrial inner membrane enzymes, but we could identified three cross reacting sequences on the bCS enzyme. The three recognized sequences show only a limited homology with hCS.

Investigation of pathologic autoimmunity in the rhG1-induced arthritis (GIA) model

1. With the intraperitoneal injection of rhG1 we could induce arthritis in T cell receptor transgenic mouse lines, which $CD4^+$ T cells recognize the dominant epitope on the G1 domain of the proteoglycan molecule. Two founders with high TCR expression were backcrossed into genetically susceptible BALB/c strain, and that way the TCR-TgA and TCR-TgB lines were constructed. During the side-by-side immunizations profound differences between the two lines appeared. TCR-TgA mice exhibited accelerated and more severe arthritis than TCR-TgB mice in response to rhG1 immunization. The clinical phenotype and disease characteristics TCR-TgB were more similar to those found in WT BALB/c mice.
2. Serum parameters correlated with the clinical phenotype: TCR-TgA mice exhibited significantly more antigen-specific antibodies and inflammatory cytokines when compared to TCR-TgB littermates.
3. We found also differences when we characterized the lymphocyte subpopulations in the two strain. TCR-TgB mice expressed approximately twice as much TCR as TCRTgA mice. Activated T cells ($CD25^{high}$, $CD44^+$) were represented in higher ratio in the lymphoid organs of TCR-TgA mice when compared to TCR-TgB mice. We got controversial results with the examination of Treg (Tregs play important role in the regulation of tolerance/autoimmunity) cells in the two strains: more Tregs were observed in TCR-TgA mice than in

TCR-TgB mice during the entire immunization period. The elevated proportion of B cells in the lymphoid organs of TCR-TgA mice probably correlates with the higher concentration of antibodies and elevated number of activated T cells (through the more effective antigen presentation).

4. With the use of phospho-flow technique we detected accelerated cell signaling in TCR-TgB mice. After in vitro antigen stimulation TCR related cell signaling molecules (ZAP-70, p38) were phosphorilated on higher level in TCR-TgB mice.
5. The extremely 'strong' TCR signal, due probably to higher TCR expression, led to in vivo T cell apoptosis and diminished arthritis in TCR-TgB mice.

PUBLICATIONS

List of publications related to the thesis [IF: 21.708]:

1. **Olasz, Katalin**; Boldizsar, Ferenc; Kis-Toth, Katalin; Tarjanyi, Oktavia; Hegyi, Akos; van Eden, Willem; Rauch, Tibor; Mikecz, Katalin; Glant, Tibor: *T cell receptor (TCR) Signal Strength Controls Arthritis Severity in Proteoglycan-Specific TCR Transgenic Mice.*
Clin. Exp. Immunol. 67(2): 346-55., 2012.
IF: 3.134*

2. Glant TT, Radacs M, Nagyeri G, **Olasz K**, Laszlo A, Boldizsar F, Hegyi A, Finnegan A, Mikecz K.: *Proteoglycan-induced arthritis and recombinant human proteoglycan aggrecan G1 domain-induced arthritis in BALB/c mice resembling two subtypes of rheumatoid arthritis.*
Arthritis Rheum. 63(5): 1312-21., 2011.
IF: 8.435*

3. Czömpöly T, **Olasz K**, Nyárády Z, Simon D, Bovári J, Németh P.: *Detailed analyses of antibodies recognizing mitochondrial antigens suggest similar or identical mechanism for production of natural antibodies and natural autoantibodies.*
Autoimmun Rev. 7(6):463-7., 2008.
IF: 5.371

4. Czömpöly T, **Olasz K**, Simon D, Nyárády Z, Pálinkás L, Czirják L, Berki T, Németh P.: *A possible new bridge between innate and adaptive immunity: Are the anti-mitochondrial citrate synthase autoantibodies components of the natural antibody network?*
Mol Immunol. 43(11):1761-8., 2006.
IF: 4.768

Other publications [IF: 30.361]:

5. Nagyeri G, Radacs M, Ghassemi-Nejad S, Tryniszewska B, **Olasz K**, Hutas G, Gyorfy Z, Hascall VC, Glant TT, Mikecz K.: *TSG-6 protein, a negative regulator of inflammatory arthritis, forms a ternary complex with murine mast cell tryptases and heparin.*
J Biol Chem. 2011 Jul 1;286(26):23559-69., 2011.
IF: 5.328

6. Czömpöly T, Lábadi A, Kellermayer Z, **Olasz K**, Arnold HH, Balogh P.: *Transcription factor Nkx2-3 controls the vascular identity and lymphocyte homing in the spleen.*
J Immunol. 186(12):6981-9., 2011. IF: 5.745*

7. Nesterovitch AB, Szanto S, Gonda A, Bardos T, Kis-Toth K, Adarichev VA, **Olasz K**, Ghassemi-Najad S, Hoffman MD, Tharp MD, Mikecz K, Glant TT.: *Spontaneous insertion of a b2 element in the ptpn6 gene drives a systemic autoinflammatory disease in mice resembling neutrophilic dermatosis in humans.*
Am J Pathol. 178(4):1701-14., 2011.
IF: 5.224*

8. Boldizsar F, Kis-Toth K, Tarjanyi O, **Olasz K**, Hegyi A, Mikecz K, Glant TT.: I*mpaired activation-induced cell death promotes spontaneous arthritis in antigen (cartilage proteoglycan)-specific T cell receptor-transgenic mice.*
Arthritis Rheum. 62(10):2984-94., 2010.
IF: 8.435

9. Angyal A, Egelston C, Kobezda T, **Olasz K**, László A, Glant TT, Mikecz K.: *Development of proteoglycan-induced arthritis depends on T cell-supported autoantibody production, but does not involve significant influx of T cells into the joints.*
Arthritis Res Ther. 12(2): R44., 2010.
IF: 4.357

10. Bovári J, Czömpöly T, **Olasz K**, Arnold HH, Balogh P.: *Complex organizational defects of fibroblast architecture in the mouse spleen with Nkx2.3 homeodomain deficiency.*
Pathol Oncol Res. 2007;13(3):227-35.
IF: 1.272

ACKNOWLEDGEMENTS

First of all I would like to thank my supervisors **Prof. Péter Németh** and **Dr. Ferenc Boldizsár** for giving me the possibility to work at the Institute of Immunology and Biotechnology. I would also like to thank them for leading me during this scientific endeavor and for having faith in this project.

I would like to thank **Prof. Dr. Tibor Glant** for giving me the possibility to work for two years at the Rush University at Chicago, and for introducing me the experimental animal model of rheumatoid arthritis, and several modern laboratory technics.

I greatly appreciate the technical help and lead in the epitope mapping technique of **Dr. Tamás Czömpöly** and **Dr. Diána Simon**. I would also like to thank for **Dr. Zoltán Nyárády** for the help with bioinformatics realted to the thesis.

I would like to thank **Prof. László Czirják** and **Prof. György Füst** and **Dr. Zoltán Prohászka** for the autoimmune patient's sera and for the Finnish blood donor serum samples, respectively.

I would like to thank **Dr. Alessandra Luzzago** for providing us the filamentous phage random peptide library and the lambda phage display vector.

I would like to thank **Prof. Ferencz Hudecz** and **Szilvia Bősze** for the multi-pin peptide synthesis.

I would also like to thank for my husband **Ákos Hegyi** for supporting my work during these years, and for the technical help in Chicago.

Finally, I would like to thank all members of Department of Immunolgy and Biotechnology and the members of Rush University Medical Center for helping me in this work.